Interactions between two-dimensional composite vector solitons carrying topological charges

Ziad H. Musslimani,[1] Marin Soljačić,[2] Mordechai Segev,[3] and Demetrios N. Christodoulides[4]
[1]*Department of Applied Mathematics, University of Colorado, Campus Box 526, Boulder, Colorado 80309-0526*
[2]*Department of Physics, Massachusetts Institute of Technology, Cambridge, Massachusetts 02139*
[3]*Physics Department and Solid State Institute, Technion—Israel Institute of Technology, 32 000 Haifa, Israel and Department of Electrical Engineering, Princeton University, Princeton, New Jersey 08544*
[4]*Department of Electrical Engineering and Computer Science, Lehigh University, Bethlehem, Pennslyvania 18015*
(Received 6 December 2000; published 23 May 2001)

We present a comprehensive study of interactions (collisions) between two-dimensional composite vector solitons carrying topological charges in isotropic saturable nonlinear media. We numerically study interactions between such composite solitons for different regimes of collision angle and report numerous effects which are caused solely by the ''spin'' (topological charge) carried by the second excited mode. The most intriguing phenomenon we find is the delayed-action interaction between interacting composite solitons carrying opposite spins. In this case, two colliding solitons undergo a fusion process and form a metastable bound state that decays after long propagation distances into two or three new solitons. Another noticeable effect is spin-orbit coupling in which angular momentum is being transferred from ''spin'' to orbital angular momentum. This phenomenon occurs at angles below the critical angle, including the case when the initial soliton trajectories are in parallel to one another and lie in the same plane. Finally, we report on shape transformation of vortex component into a rotating dipole-mode solitons that occurs at large collision angles, i.e., at angles for which scalar solitons of all types simply go through one another unaffected.

DOI: 10.1103/PhysRevE.63.066608 PACS number(s): 42.81.Dp

I. INTRODUCTION

Soliton interactions are one of the most fascinating features of nonlinear sciences. They are universal, displaying features common to all solitons, in spite of the diversity of the physical systems in which solitons are found [1]. The underlying reason for this universality is the fact that solitons can be viewed as bound states of their own induced potential well or, in nonlinear optics, as modes of their own induced waveguide [2]. The simplest case arises when the self-induced waveguide (potential well) has only one mode populated, in which case the soliton is a ''single-mode'' entity. In this vein, collisions of single-mode solitons can be viewed intuitively as interactions between guided modes of adjacent waveguides, and the interaction outcome is determined by the relation between the collision angle and the (complementary) critical angle (θ_c) for total internal reflection in each waveguide. Experimentally, collisions between single-mode solitons have been studied in detail, demonstrating fully elastic collisions between Kerr solitons [3], almost-elastic collisions between solitons in saturable nonlinear media interacting at angles above the critical angle [4], and inelastic collisions between solitons that yield fusion [4–7], fission [7], annihilation [7], and spiraling [8].

More than a decade ago, multimode (or composite) solitons were proposed: First in the temporal domain [9], and later on in the spatial domain [10]. The discovery of solitons in noninstantaneous nonlinear media has opened up a wide range of possibilities in terms of demonstrating composite solitons [11] (see details and citations in Ref. [1]). And indeed composite bright-dark [12] and multimode solitons [13] were experimentally observed. Theoretical and experimental papers on interactions of composite solitons followed soon thereafter, reporting on shape transformations upon collision [14], and on a bound state between two vector solitons, each being a composite dark-bright soliton pair [15]. In all of these studies the solitons considered were of (1+1)-dimensional type. Recently, however, we have proposed the possibility of generating (2+1)-dimensional multimode composite solitons in which at least one component carries topological charge [16]. Later on, two-dimensional (2D) dipole-type composite solitons were suggested [17] and experimentally observed [18,19]. Very recently, a rotating propeller-type composite solitons was predicted and observed [20]. In this composite soliton, the second mode is a dipole and it is rotating in unison with the (slightly elliptic) fundamental mode during propagation.

In this paper, we present a detailed theoretical study of collisions between (2+1)D composite solitons carrying topological charges. Depending on the collision angle, these 3D interactions exhibit rich behavior upon collision, such as fusion, fission and spiraling. In particular, the collision gives rise to an on-going spiraling process in which some of the collision products spiral around each other. The spiraling occurs even when the solitons are initially launched with trajectories in the same plane, or even more intriguing, when they are launched in parallel to one another. In this latter case, the interaction is a clear manifestation of spin-orbit interaction. We also observed a very intriguing phenomenon of soliton interactions: two soliton colliding at a given scattering angle, undergo a fusion process, and after some propagation distance, the fusion product breaks up and two (or sometimes three) new solitons emerge. This ''delayed action'' phenomena turns out to be robust against perturbations.

This paper is organized as follows. In Sec. II we reiterate the existence of composite solitons carrying topological charges both for the step index and saturable nonlinearities.

To facilitate the understanding, we recall in Sec. III known results from interactions between scalar two-dimensional cylindrically symmetric solitons. Then, we present in Sec. IV a detailed study, based on numerical simulations, of interactions between vector solitons carrying identical topological charges and report on new effects of spin-orbit coupling and shape transformation of the vortex component into a dipole. In Sec. V we simulate interactions between multimode solitons carrying opposite spin in which we find new phenomena: a three-dimensional delayed-action interaction, and energy exchange between rotating dipole solitons, both of which occur for solitons colliding at an angle that is slightly below or close to the critical angle. We conclude in Sec. VI.

II. COMPOSITE (2+1)D SOLITONS CARRYING TOPOLOGICAL CHARGES

In what follows, we review our results [16] on composite solitons carrying topological charges, i.e., multicomponent two-dimensional [(2+1)D] vector solitons for which at least one component carries topological charge [21]. We do not consider here composite solitons in which both fields carry nonzero topological charges [22]. To make our theoretical study as analytic as possible, we draw on the so-called thresholding nonlinearity, and employ the *self-consistency* principle presented in Ref. [10]. We seek composite solitons for which at least one mode carries topological charge. Following this analytic study, we present below a numerical study of composite solitons in realistic saturable nonlinearity.

We start from the normalized nonlinear Schrödinger (NLS) equations [16,17]

$$i\frac{\partial\psi_j}{\partial z}+\nabla^2\psi_j+\delta n(I)\psi_j=0, \tag{1}$$

where ψ_j, $j=0,1$ are the envelopes of two interacting beams; z is the normalized propagation distance and $\nabla^2=\partial^2/\partial x^2+\partial^2/\partial y^2$ is the normalized transverse Laplacian. Equations (1) describe two coupled beams in an optical medium with a *normalized* nonlinear refractive index change $\delta n(I)$ and total intensity $I=\Sigma_{j=0}^{1}|\psi_j|^2$. We seek multicomponent soliton solutions to Eqs. (1), for which each component ψ_j carries a topological charge m_j in the form

$$\psi_j(r,\varphi,z)=u_j(r)\exp(i\mu_j z+im_j\varphi), \quad j=0,1, \tag{2}$$

μ_j being the propagation constants of the vector constituents. The simplest case occurs when $m_0=0$ and $m_1=\pm 1$. We denote such solutions by $(0,\pm 1)$. In other words, the first mode has radial symmetry (circular geometry) with maximum peak intensity at the origin, while the second mode is of the vortex type (doughnut geometry). Substituting Eq. (2) into Eq. (1) we find

$$\frac{d^2u_j}{dr^2}+\frac{1}{r}\frac{du_j}{dr}-\frac{m_j^2}{r^2}u_j+\delta n(I)u_j=\mu_j u_j, \tag{3}$$

with the refractive index change given as

$$\delta n(I)=\delta n(u_0^2+u_1^2). \tag{4}$$

System (3) is a nonlinear eigenvalue problem with μ_j being the eigenvalues and ψ_j are the corresponding eigenfunctions. Equations (3) are supplemented with the following boundary conditions:

$$\begin{gathered} u_j(r)\to 0 \quad \text{as} \quad r\to+\infty, \\ u_0(0)=u_{\text{peak}}, \quad u_0'(0)=0, \quad u_1(0)=0. \end{gathered} \tag{5}$$

A. Step-index nonlinearity: A fully solvable model

The step-index or threshold nonlinearity is defined by a *normalized* nonlinear refractive index change $\delta n(I)$ being zero for $I<I_{\text{th}}$ and constant $\delta n_0=1$ otherwise. The solutions to system (3) with boundary conditions given in Eq. (5) are

$$u_j(r)=\begin{cases} \eta_j J_{m_j}(\kappa_j r), & 0\leqslant r\leqslant a \\ \eta_j \dfrac{J_{m_j}(\kappa_j a)}{K_{m_j}(\sqrt{\mu_j}a)}K_{m_j}(\sqrt{\mu_j}r), & r\geqslant a, \end{cases} \tag{6}$$

where $\kappa_j^2\equiv\delta n_0-\mu_j>0$ and $\mu_j>0$; J_{m_j} (K_{m_j}) are the regular (modified) Bessel functions of the first (second) kind of order m_j; and a is the normalized radius (the so-called V number [23]) of the induced waveguide. The propagation constants satisfy

$$\frac{\sqrt{\mu_j}K_{m_j-1}(\sqrt{\mu_j}a)}{K_{m_j}(\sqrt{\mu_j}a)}+\frac{\kappa_j J_{m_j-1}(\kappa_j a)}{J_{m_j}(\kappa_j a)}=0. \tag{7}$$

The eigenvalue Eq. (7) describes the eigenmodes of a weakly guiding step-index fiber for which the polarization states can be found in Ref. [23]. We impose the self-consistency condition [2] on the vector components, i.e., the total intensity at the margins of the induced waveguide is equal to the threshold intensity

$$I_{\text{th}}=\eta_0^2J_0^2(\kappa_0 a)+\eta_1^2J_1^2(\kappa_1 a). \tag{8}$$

Solving Eq. (7) together with the self-consistency condition (8) we find multiple branches of existence range of composite vector solitons as shown in Fig. 1. Their total intensity exhibit different shapes on different groups of branches [24]. In branches I and II, the cross section of the total intensity changes by increasing η_1 ($\eta_1=0$ being the scalar case), from circular to a ring geometry (or the intensity cross section changes from single to double ''humps'') on branch I, and from a single ring to two concentric rings geometry (three to four ''humps'') on branch II. In Fig. 2 we show typical examples of such composite solitons profiles taken from branches I and II [corresponding to Figs. 1(b) and 1(d)]. On the mixed branch, however, we observe a transition from single to double humps then to four humps in the intensity cross sections taken through the origin of the beam [see Fig. 1(c) and specific examples in Figs. 3(a)–3(c)].

Further increasing η_1, we find a narrow range of parameters, where the induced waveguide resembles to a *hollow*

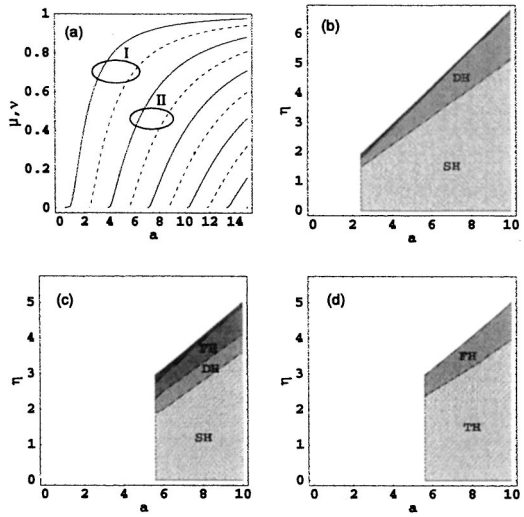

FIG. 1. (a) Propagation constants μ_0 (solid) and μ_1 (dashed) as a function of the normalized radius a of the induced waveguide (the V number); (b)–(d) existence regions for composite (0,1) solitons at different branches: (b) branch I, (c) mixed branch, and (d) branch II.

fiber [see Fig. 3(d)]. This region corresponds to the dark area in Fig. 1(c) and exists also in branches I and II, although the region is narrower [Figs. 1(b), 1(d)].

B. Vector (2+1)D solitons in saturable nonlinearity

In this section we study the existence of composite solitons in a true saturable nonlinearity which represents, e.g., nonlinearities in an isotropic homogeneously broadened two-level system. In this case, Eqs. (1) describe the interaction of

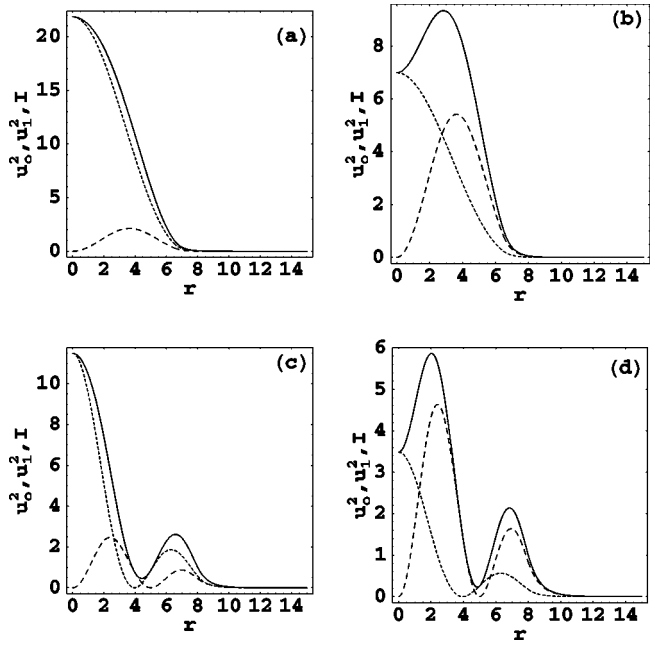

FIG. 2. u_0^2 (doted), u_1^2 (dashed), and total intensity I (solid). The parameters are (a) $a=6.5$, $\eta_1=2.5$ (branch I); (b) $a=6.5$, $\eta_1=4$ (branch I); (c) $a=8$, $\eta_1=2.7$ (branch II); and (d) $a=8$, $\eta_1=3.7$ (branch II).

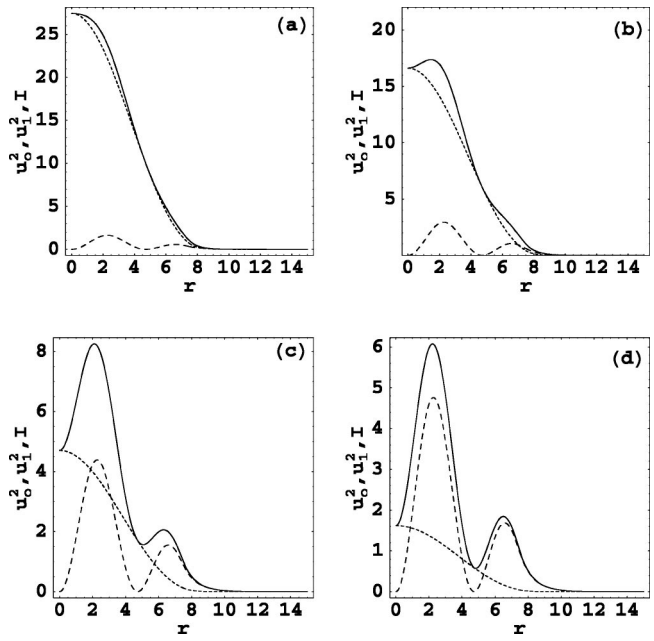

FIG. 3. As in Fig. 2 with parameters $a=7.5$ (mixed branch) and $\eta=2.2$ (a), 2.95 (b), 3.6 (c), and 3.75 (d).

two incoherently coupled beams in saturable self-focusing nonlinearity with normalized nonlinear refractive index change given by

$$\delta n(I) = -\frac{1}{1+I}, \quad I = |\psi_0|^2 + |\psi_1|^2. \tag{9}$$

The solutions to system (3) with $\delta n(I)$ given in Eq. (9) that satisfy boundary conditions (5) exhibit the same features as the solitons of the thresholding nonlinearity discussed before. Using a relaxation method, we find the wave functions of composite two-component solitons (as shown below), and indeed they have the same features as the solitons of the thresholding nonlinearity, including the multihump structure, except that now one can use the results to study stability and collisions. In Fig. 4 we show a typical solution with $u_{\text{peak}}=2$ and $\max(u_1)=0.64$.

Now, we discuss stability of these solutions. We find (numerically) that, at least in the single hump case, these structures are stable against deviations of at least 2% in initial amplitudes and at least 5% in terms of the relative displacement of the vector components. We have checked all of these perturbations within a propagation distance in excess of 100 physical diffraction lengths. Thus, we can safely conclude that at least the single hump composite solitons in a true saturable nonlinearity should be observable. Similar results were found in Ref. [25], and confirm that, although such solitons might be ultimately mathematically unstable, the saturation of the nonlinearity arrests the instability and the composite solitons should survive for very large propagation distances. We emphasize that these results do not contradict experimental findings [19,26] with the photorefractive screening nonlinearity [27,28]. In these experiments, the vortex-type composite solitons are found to break up within one diffraction length. This break up is a direct result of the

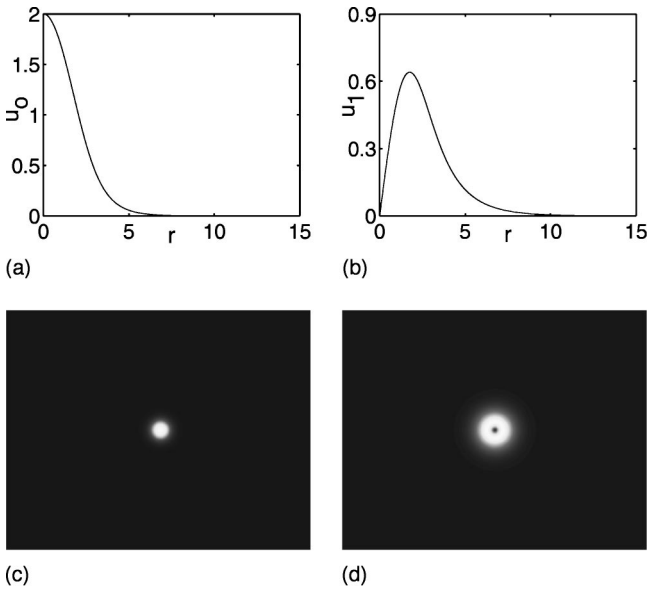

FIG. 4. Numerical solutions to system (3) obtained for $u_{\text{peak}}=2$ and $\max(u_1)=0.64$. (a), (b) are the profiles of $u_0(r)$ and $u_1(r)$, respectively. (c), (d) are the cross section in the (x,y) plane of the first (u_0) and the second mode u_1, respectively.

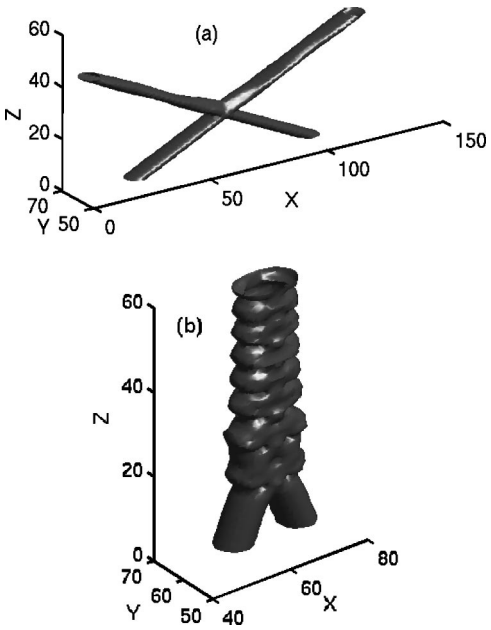

FIG. 5. Interactions of two circular *scalar* solitons ($\psi_1\equiv 0$ and ψ_0 carries zero charge). (a) above the critical angle and (b) below the critical angle.

anisotropy of the photorefractive screening nonlinearity, for which the induced waveguide is different for the two transverse directions [29,30]. However, in isotropic saturable nonlinear media, such as, for example, atomic vapors [5,31], we expect that vortex-type composite solitons will be stable for propagation distances in excess of 100 diffraction length, and will easily facilitate collision experiments.

III. INTERACTIONS BETWEEN (2+1)D SCALAR SOLITONS

For completeness, we first recall known results from interactions between cylindrically symmetric scalar solitons in saturable self-focusing nonlinear media [32]. Such solitons are solutions of a single NLS equation with $\psi_1\equiv 0$ [1], i.e.,

$$i\frac{\partial\psi_0}{\partial z}+\frac{1}{2}\nabla^2\psi_0-\frac{\psi_0}{1+|\psi_0|^2}=0. \tag{10}$$

When two scalar solitons with circular cross section collide with trajectories in the same plane and at angle $\theta>\theta_c$ then they pass through each other unaffected (maintaining their circular shape) [4], whereas they undergo fusion or fission [5–7] for $\theta<\theta_c$ (Fig. 5). This, in turn, serves as a definition of the critical angle θ_c [33].

IV. COLLISIONS BETWEEN (2+1)D IDENTICAL MULTIMODE VECTOR SOLITONS CARRYING TOPOLOGICAL CHARGES

In this section, we present a detailed numerical study of collisions between two-dimensional *identical* (having the same structure) composite solitons carrying topological charges for different regimes of collision angle. The collision process between such composite solitons gives rise to a series of very interesting phenomena, such as spin-orbit coupling, and many other effects that will be discussed separately. These interaction features should occur in any isotropic saturable self-focusing nonlinear media, yet in our study we consider two beams interacting in a medium with normalized nonlinear refractive index change $\delta n(I)$ given in Eq. (9) where I is the total (time-average) intensity. The slowly varying envelope functions of the two interacting beams $\psi_j, j=0,1$ satisfy two coupled normalized nonlinear Schrödinger (NLS) equations [16,17] given in Eq. (1). These equations admit the following conservation laws:

$$E_j=\int\int|\psi_j|^2dxdy \quad j=0,1, \tag{11}$$

which represents the power of each component; in addition the transverse momentum **P** and the angular momentum **L** are conserved

$$\mathbf{P}=\int\int\mathbf{p}dxdy, \quad \mathbf{L}=\int\int\mathbf{r}\times\mathbf{p}dxdy, \tag{12}$$

where **r** is the transverse vector coordinate and **p** is the momentum density given by

$$\mathbf{p}=\frac{i}{2}\int\int\left(\sum_{j=0}^{1}\psi_j\nabla\psi_j^*-\text{c.c.}\right)dxdy, \tag{13}$$

These conserved quantities bear much importance because they relate solitons to particles.

To study collisions between composite solitons carrying topological charges, we perform extensive numerical simulations for which we launch in the (x,z) plane two vector

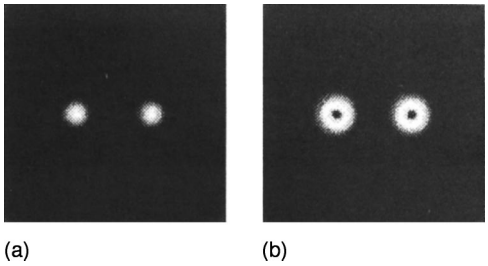

FIG. 6. Cross sections at $z=0$ (input) of the fundamental mode intensity $|\psi_0|^2$ (a) and of the first excited mode intensity $|\psi_1|^2$ (b).

soliton pairs, each of which comprises of a circular component and a doughnut (vortex) component. Here, we consider only single-hump composite solitons which were shown numerically [16] to be stable for propagation distances in excess of 100 physical diffraction lengths.

A. Collisions above the critical angle

We simulate Eq. (1) with initial condition given by ($j=0,1$):

$$\psi_j^{\text{initial}} = \sum_{s=\pm 1} \psi_j(\mathbf{r}+s\mathbf{r}_0; z=0)e^{is\vartheta x}, \tag{14}$$

where 2ϑ is the collision angle [34] (or twice the soliton transverse velocity) and $2|\mathbf{r}_0|$ is the separation between the centers of the *identical* composite solitons. Initially, (at $z=0$) the vector solitons lie entirely on the x axis (as shown in Fig. 6). In Fig. 7, we show interactions between two 13 μm full width at half maximum (FWHM) (of I) single-hump identical vector solitons (each having $m_0=0$ and $m_1=+1$) colliding at angle $\theta \approx 2° > \theta_c$. On first glance, it seems as if both components interact like scalar solitons do at angles $\theta > \theta_c$, i.e., their trajectories cross each other. However, here the ψ_1 components acquire after the collision a *rotating dipole-type* shape [Figs. 8(c) and 8(d)] whereas the ψ_0 components attain *elliptical* cross section [Figs. 8(a) and 8(b)]. Such rotating dipole solitons were recently observed in photorefractive materials [20]. The ψ_0 and ψ_1 components of both solitons rotate simultaneously (''phase locked''), each around its own center of mass in a clockwise direction. This shape transformation into dipole upon collision and rotation are *solely* due to the spin carried by the solitons and are *not* observed with scalar solitons.

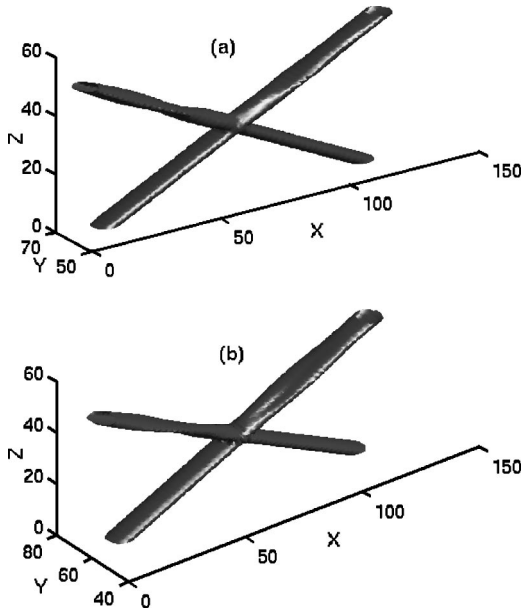

FIG. 7. Interactions between two identical composite vector solitons (each carries identical topological charges $m_0=0$ and $m_1=+1$) colliding at angle $\theta \approx 2° > \theta_c$, with $|\psi_0(0)|^2=4$ and $\max(|\psi_1|^2)=0.64$. The initial separation between the components is 50.5 μm. (a) shows the ψ_0 components and (b) the ψ_1 components.

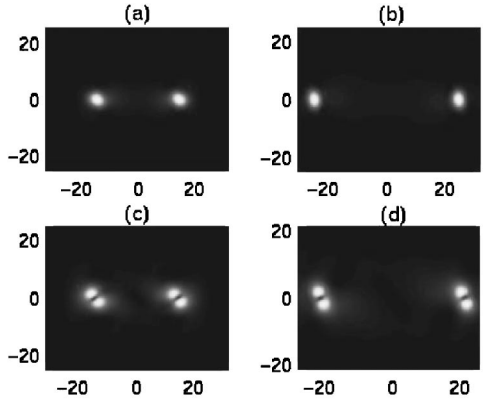

FIG. 8. Snapshots of the fundamental mode intensity $|\psi_0|^2$ at $z=32$ (a) and $z=38$ (b). Similarly, a snapshots of the first excited mode intensity, $|\psi_1|^2$ is shown at $z=32$ (c) and $z=38$ (d).

B. Collisions close to the critical angle

As we decrease the collision angle θ to an ''intermediate'' value, e.g., $\theta \approx 0.66° \approx \theta_c$, we observe a qualitative change in the interaction picture (Fig. 9). In this case, the two interacting vector solitons undergo a *fission* process which ends up in creation of four pairs of components, in which each pair is self-trapped separately. The two ''outer'' pairs travel almost like free particles, whereas the ''inner'' pairs show strong pulsation and after propagating at close proximity for some distance, they eventually escape away from one another. Interestingly, although the initial paths

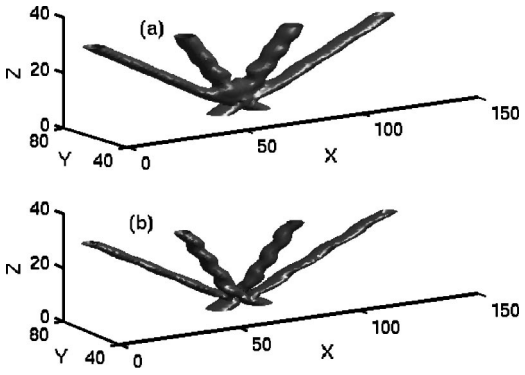

FIG. 9. As in Fig. 7 but for collision angle $\theta \approx 0.66° \approx \theta_c$.

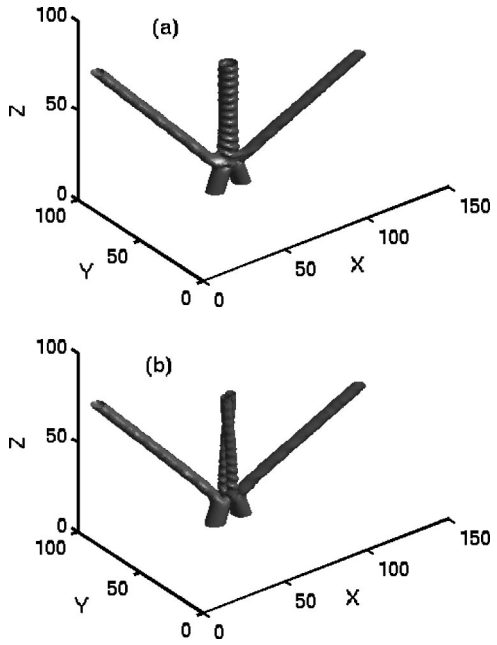

FIG. 10. As in Fig. 7 but for a collision angle $\theta \approx 0.12° < \theta_c$.

(before collision) of the composite solitons were solely in the (x,z) plane, the emerging four soliton pairs do not lie in that plane anymore, but rather in a plane that is tilted clockwise with respect to (x,z) by an angle of 5.7° in the direction of the co-rotating topological charges. This tilt of the plane of propagation is contrary to the $\theta > \theta_c$ case in which the emerging soliton paths are *always* in the (x,z) plane.

C. Collisions below the critical angle: Spin-orbit coupling

Further decreasing the collision angle *below* the critical angle, e.g., $\theta \approx 0.12°$, we observe the production of three vector solitons which are completely decoupled from each other (Fig. 10). The resulting solitons propagate in a plane that is tilted by an angle 28.65°. In the outer two pairs ψ_0 and ψ_1 both occupy the lowest mode of their jointly induced waveguide. On the other hand, for the inner soliton components, ψ_0 and ψ_1 occupy self-consistently the first and second modes of their jointly induced potential. Furthermore, the inner composite soliton emerging from the collision develops complicated dynamics: its ψ_0 constituent initially shows pulsation that gradually evolved into rotation around its own center of mass [Fig. 10(a)]. This dynamics relaxes after some distance. Surprisingly, the emerging ψ_1 field has the form of a dipole, and exhibits *stable spiraling* [35] for all propagation distances in access [Fig. 10(b)]. Figure 11 shows a magnified version of the propagation dynamics displayed in Fig. 10(b), for a longer propagation distance (up to $z = 232$). We emphasize that this spiraling of the middle ψ_1 component, occurs even though the initially launched solitons had trajectories in the same plane. The spiraling occurs because some of the angular momentum carried by the spin $[\exp(im\varphi)]$ is transferred to orbital angular momentum. This is a clear manifestation of *spin-orbit* interaction between solitons. This generic behavior appears for all collisions with $\theta < \theta_c$ including $\theta = 0$ (when the solitons are launched in parallel). In other words, the spiraling behavior of the emerging inner ψ_1 dipole component appears also in the case of fully parallel-launched solitons. In the most counterintuitive manner we find that solitons launched in parallel with one another undergo fission, and one of the fission product exhibits spiraling. All this fascinating dynamics occurs just because the input solitons are carrying ''spin.''

FIG. 11. A magnified version of the dynamics displayed in Fig. 10(b).

Finally, we note that the emerging solitons, for any collision angle $\theta \lesssim \theta_c$, lie in a plane tilted with respect to the plane of incidence (x,z). The tilt angle increases with decreasing θ, and at $\theta = 0$ reaches 37°. If all the colliding vector solitons have $m = -1$, then the plane of the emerging solitons is tilted in an opposite direction, and all the rotation dynamics presented above, including the spiraling, occurs in reverse (anticlockwise) direction.

Before closing this section, we revisit the particlelike quantities that characterize the solitons: power E_j of each component and total angular momentum L. To this end, we consider for example the collision depicted in Fig. 5. In the first stage, before the collision takes place (up to $z = 10$), E_j and L decrease very slowly at a rate of 0.003% per diffraction length (which is set up by our numerical accuracy). In the second stage, during which the solitons strongly overlap and interact, E_j and L decrease at a higher rate (this is where radiation modes are highly excited) of 0.05% per diffraction length. In the final stage, after the collision has ended, only the inner spiraling dipole and its ψ_0 companion continue to loose power and angular momentum at almost the same rate as before.

The long term prospect of evolution of the inner solitons seems to be that the dipole eventually coalesces to a circular shape and both components occupy the lowest mode of their jointly induced waveguide. It seems (numerically) that this behavior is characteristic of all such interactions of composite solitons carrying topological charge. To conclude this section, we have studied interactions between composite solitons carrying identical topological charges for different values of collision angles. We report on several effects which are caused by the ''spin'' carried by the second excited mode such as shape transformation (a vortex into a dipole), fusion and fission. Perhaps the most noticeable effect is the observation of spin-orbit interaction which occurred at angles below the critical angle, including when the initial soliton trajectories were in parallel to one another and lie in the same plane.

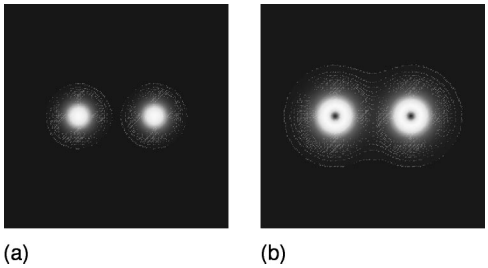

FIG. 12. Cross sections at $z=0$ (input) of the fundamental mode intensity $|\psi_0|^2$ (a) and of the first excited mode intensity $|\psi_1|^2$ (b).

V. COLLISIONS BETWEEN (2+1)D COMPOSITE SOLITONS CARRYING OPPOSITE TOPOLOGICAL CHARGES

In this section, we report on a new collision effect: delayed-action interaction. It occurs when two composite solitons carrying topological charges $m_1=\pm 1$ collide, and form a bound state that has a prolonged ''lifetime'' (propagation distance) of about 35, yet this bound state decays at some point into two or three new vector solitons, that are fundamentally different than the original input solitons (see Fig. 15 for a schematic representation of the phenomena). In addition, we report in this section on energy exchange between rotating dipole solitons that emerge as a result of collision between vortex type vector solitons.

A. Collisions above the critical angle

We have simulated Eq. (1) with the initial condition (see Fig. 12) given by Eq. (14). In this case, the first vector soliton is of the (0,1) type, i.e., ψ_0 has charge $m_0=0$ and ψ_1 has charge $m_1=+1$ whereas the second vector is of the (0, -1) type (i.e., ψ_0 has $m_0=0$ and ψ_1 has charge $m_1=-1$). At a very large collision angle ($\theta\approx 2\,^\circ > \theta_c$) the two vector solitons go through each other (see Fig. 13). The first component (ψ_0) attains an elliptical shape whereas the ψ_1 component undergoes a shape-transformation, from vortex type to a rotating dipole. Each single component that constitute the ψ_1 field starts rotating (right after they collide) in an opposite direction, one in a clockwise and the other in an anticlockwise directions [see Fig. 13(b)]. This shape transformation interaction resembles the interaction between composite solitons with corotating vortices (see Sec. IV). However, as we decrease the angle, all the interaction picture changes dramatically and attains features that were never observed before.

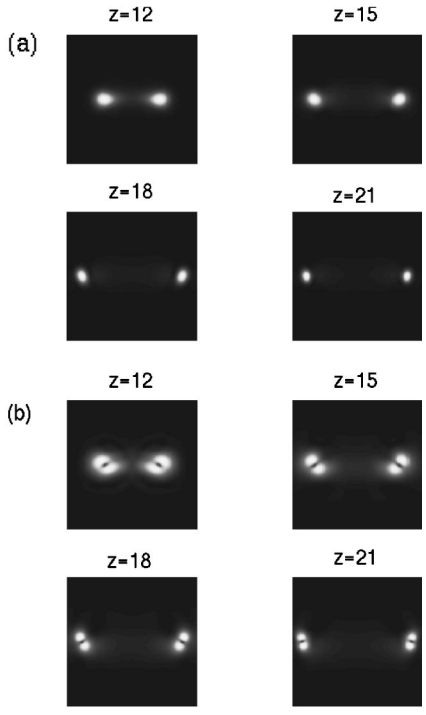

FIG. 13. Interactions of two vortex-type composite solitons with (0,1) and (0,-1) structure colliding at angle $\theta\approx 2\,^\circ > \theta_c$, with $|\psi_0(0)|^2=4$ and $\max(|\psi_1|^2)=0.64$. The initial separation between the components is 13 (in a dimensionless units). (a) shows the ψ_0 components and (b) the ψ_1 components.

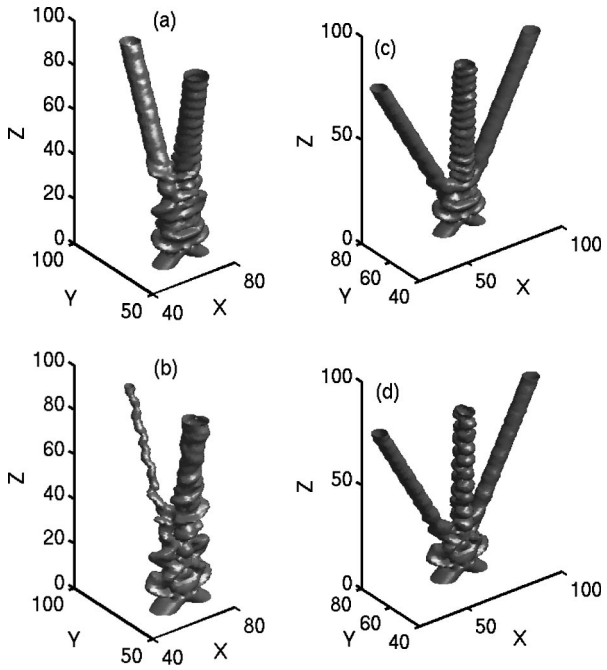

FIG. 14. Interactions of two composite solitons colliding at $\theta\approx 0.37\,^\circ < \theta_c$, with $|\psi_0(0)|^2=4$ and $\max(|\psi_1|^2)=0.64$. (a), (b) show the ψ_0, ψ_1 components. (c),(d) same as (a),(b) but with deviations of 3% in initial amplitudes.

B. Collisions close to the critical angle: Delayed-action interaction

When two identical composite solitons of opposite ''spins'' collide at an angle $\theta\approx 0.37\,^\circ < \theta_c$, then both vector

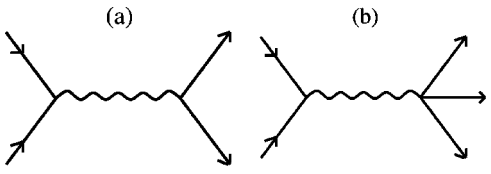

FIG. 15. Schematic representation of the two delayed action examples shown in Fig. 14. Two vector solitons collide, a metastable bound state forms, and after many diffraction lengths, the bound state decays into new vector solitons. (a) corresponds to Figs. 14(a), 14(b), whereas (b) refers to Figs. 14(c), 14(d).

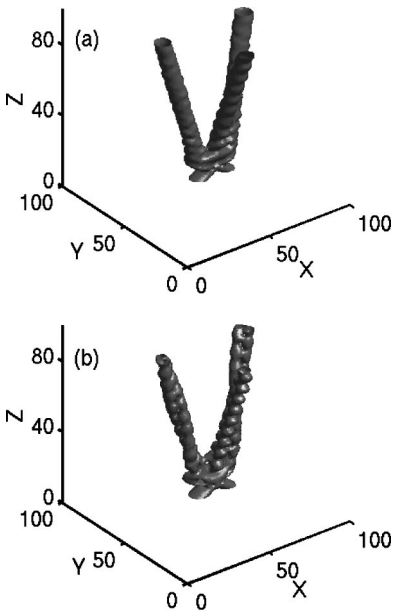

FIG. 16. Interactions of two composite solitons colliding at angle $\theta \approx 0.48° > \theta_c$, with $|\psi_0(0)|^2 = 4$ and $\max(|\psi_1|^2) = 0.64$. The initial separation between the components is 13 (in a dimensionless units). (a) shows the ψ_0 components and (b) the ψ_1 components.

constituents undergo a fusion process and form a resonant bound state that has a prolonged ''lifetime'' (propagation distance) of about 35 diffraction lengths. When this metastable bound state eventually disintegrates, it gives rise to new vector soliton states with trajectories that lie in a plane almost orthogonal to the initial plane (Fig. 14 and the schematic presentation in Fig. 15).

This delayed-action process resembles interaction processes between elementary particles, in which the intermediate (metastable) fusion product plays the role of a ''mediator.'' This phenomenon is observed here with solitons. We find (numerically) that the generic delayed-action interaction is robust against deviation of at least 3% in initial amplitudes. Even in its shortest scenario (when we perturb the initial soliton input), a bound metastable state still occurs, and it survives for a distance of 20 diffraction lengths. Nevertheless, the details of the delayed-action interaction process and the emerging solitons critically depend upon the initial amplitudes. In the examples depicted in Fig. 14, the input solitons differ by merely 3% in initial amplitudes, yet in one case two solitons emerge from the collision process, whereas in the other three solitons are emitted. Evidently, tiny changes in the input parameters completely change the details of the interaction.

For a collision angle of $\theta \approx 0.48°$ (which is smaller than, yet still close to, the critical angle), the soliton components undergo fission and give rise to three new vector solitons (Fig. 16). Of these emerging vector solitons, two are of the dipole type, and propagate in the (x,z), while the third is propagating in a plane that is tilted with respect to the (x,z) plane. Interestingly, the dipole vector solitons possess an oscillatory behavior: we observe an *energy exchange in between the dipole constituents*. This indicates that the relative phase between the vector constituents of the two solitons is

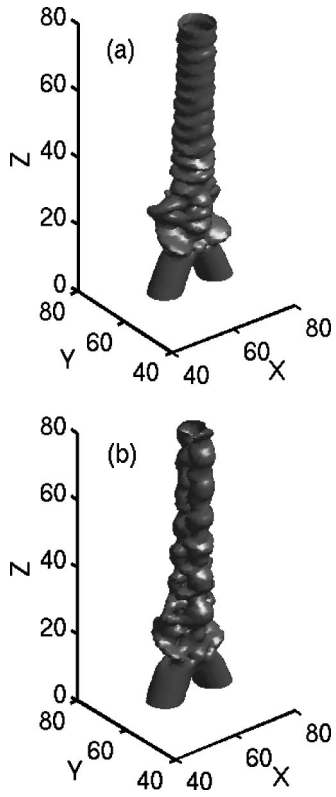

FIG. 17. Interactions of two composite solitons colliding at $\theta \approx 0.12° < \theta_c$, with $|\psi_0(0)|^2 = 4$ and $\max(|\psi_1|^2) = 0.64$. (a) show the ψ_0 and (b) ψ_1 components.

neither zero nor π. This complex shape transformation is unique to vector solitons having topological charges $m = \pm 1$ and was not found in other systems not even in the case where the vector solitons have identical ''spin.''

C. Collisions below the critical angle: Soliton fusion

As we continue to decrease the scattering angle below the critical angle, e.g., for $\theta \approx 0.12°$, the two vector soliton components merge together and form a bound state (see Fig. 17). The ψ_0 component starts rotating in a screw form until it converges to a circular shape. However, the ψ_1 components, form a rotating dipole soliton that jointly self-trap with the ψ_0 field. The ''circular'' and the dipole fields occupy the ground and the first excited states of their jointly induced potential, respectively. In essence, the collision products between composite solitons carrying opposite topological charges at angle less than the critical angle is *completely* different than in the case where the solitons have identical spins. In the later case, the vector components did *not* fuse and instead major part of the internal angular momentum (spin) was transfered into orbital angular momentum, hence no fusion was observed.

VI. CONCLUSIONS

Collisions between optical spatial solitons exhibit many fascinating and diverse aspects. The largest variety of phenomena occurs for media with saturable nonlinearity, in

which case a stationary (2+1)D propagation is possible. In all of the studies of soliton interactions, the solitons considered were either in (1+1) dimensions or with a two-dimensional cylindrical symmetry.

Here, we have proposed the possibility of generating (2+1)D multimode composite solitons in which at least one component carries topological charge. We have studied interactions between such composite solitons for different regimes and discovered numerous effects which are caused solely by the ''spin'' carried by the second excited mode, and do *not* exist for other forms of solitons. These new phenomena are absent even for the Manakov solitons and for (1+1)D multimode (composite) solitons. One example includes shape-transformation of vortex into a dipole that occurs at high scattering angles—at angles for which all solitons of all types simply go through one another unaffected. Another example is a fission process in which three vector solitons came out of two. Perhaps the most noticeable effect is the observation of spin-orbit interaction which occurred at angles below the critical angle, including when the initial soliton trajectories were in parallel to one another and lie in the same plane. In this collision process, the initial angular momentum was carried solely by the topological charge (''spin'') of each soliton (because the initial soliton trajectories are in the same plane or parallel to one another). The angular momentum is transferred, through the collision, in part to the rotation of the frame of propagation of the solitons emerging from the collision. In other words, angular momentum was transferred from the form of ''spin'' to rotations of the frame of reference, that is, to orbital angular momentum.

The most intriguing phenomenon we discovered was the ''delayed action collision'' between interacting composite solitons carrying opposite spins. This new effect has never been observed before in *any* kind of soliton bearing systems. We have seen that, in the case where the collision angle is slightly below the critical angle, two vector solitons form an unstable bound state. This bound state survives the evolution for very long distance (many diffraction lengths) until it breaks up and new vector solitons are emitted. This interaction resembles the interaction between two elementary particles in which the ''mediator'' (the fusion product) has a prolonged yet finite ''half life-time'' and eventually decays into new self-trapped entities: soliton states that diverge away from one another similar to free particles. This delayed action process is an intricate version of the (1+1)D case for which the soliton amplitudes exhibit large persistent oscillations due to internal degrees of freedom the so-called soliton internal modes [36]. In our (2+1)D case of interaction between composite solitons, this additional internal degrees of freedom take on a fascinating form, because they allow the ''storage'' of energy and angular momentum in full 3D. The result is the surprising and intriguing delayed-action interaction. Finally, it is important to note that collisions between composite solitons having identical topological charges, is fundamentally different from the case where the solitons have opposite spins. This means that one cannot tell *a priori* what will be the interaction outcome between solitons with opposite spins colliding at some given angle θ, based on collision between composite solitons having identical spins colliding at the same angle.

ACKNOWLEDGMENTS

The work of M.S., M.S., and D.N.C. was supported by the MURI program on optical spatial solitons, by the U.S. Army Research Office, the U.S. Air-Force Office of Scientific Research, and by the U.S. National Science Foundation. The work of Z.H.M. and of M.S. was supported by the Israeli Ministry of Science. Z.H.M. gratefully acknowledges the financial support of the Rothschild foundation.

[1] G. Stegeman and M. Segev, Science **286**, 1518 (1999).
[2] A. W. Snyder, D. J. Mitchell, and Y. S. Kivshar, Mod. Phys. Lett. B **9**, 1479 (1995).
[3] J. S. Aitchison, A. M. Weiner, Y. Silberberg, D. E. Leaird, M. K. Oliver, J. L. Jackel, and P. W. Smith, Opt. Lett. **16**, 15 (1991); M. Shalaby, F. Reynaud, and A. Barthelemy, *ibid.* **17**, 778 (1992); J. U. Kang, G. I. Stegeman, and J. S. Aitchison, *ibid.* **21**, 189 (1996).
[4] M. Shih and M. Segev, Opt. Lett. **21**, 1538 (1996).
[5] V. Tikhonenko, J. Christou, and B. Luther-Davies, Phys. Rev. Lett. **76**, 2698 (1996).
[6] H. Meng, G. Salamo, M. Shih, and M. Segev, Opt. Lett. **22**, 448 (1997).
[7] W. Krolikowski and S. A. Holmstrom, Opt. Lett. **22**, 369 (1997); W. Krolikowski, B. Luther-Davies, C. Denz, and T. Tschudi, *ibid.* **23**, 97 (1998).
[8] M. Shih, M. Segev, and G. Salamo, Phys. Rev. Lett. **78**, 2551 (1997); A. Buryak, Y. S. Kivshar, M. Shih, and M. Segev, *ibid.* **82**, 81 (1999).
[9] D. N. Christodoulides and R. I. Joseph, Opt. Lett. **13**, 53 (1988); M. V. Tratnik and J. E. Sipe, Phys. Rev. A **38**, 2011 (1988); M. Haelterman, A. P. Sheppard, and A. W. Snyder, Opt. Lett. **18**, 1406 (1993).
[10] A. W. Snyder, S. J. Hewlett, and D. J. Mitchell, Phys. Rev. Lett. **72**, 1012 (1994).
[11] D. N. Christodoulides, S. R. Singh, M. I. Carvalho, and M. Segev, Appl. Phys. Lett. **68**, 1763 (1996).
[12] M. Shalaby and A. J. Barthelemy, IEEE J. Quantum Electron. **28**, 2736 (1992); Z. Chen, M. Segev, T. Coskun, and D. N. Christodoulides, Opt. Lett. **21**, 1436 (1996).
[13] M. Mitchell, M. Segev, and D. N. Christodoulides, Phys. Rev. Lett. **80**, 4657 (1998).
[14] N. Akhmediev, W. Krolikowski, and A. W. Snyder, Phys. Rev. Lett. **81**, 4632 (1998); W. Krolikowski, N. Akhmediev, and B. Luther-Davies, Phys. Rev. E **59**, 4654 (1999).
[15] E. A. Ostrovskaya, Y. S. Kivshar, Z. Chen, and M. Segev, Opt. Lett. **24**, 327 (1999).
[16] Z. H. Musslimani, M. Segev, D. N. Christodoulides, and M. Soljačić, Phys. Rev. Lett. **84**, 1164 (2000); Z. H. Musslimani, M. Segev, and D. N. Christodoulides, Opt. Lett. **25**, 61 (2000).

[17] J. J. García-Ripoll, V. M. Pérez-García, E. A. Ostrovskaya, and Y. S. Kivshar, Phys. Rev. Lett. **85**, 82 (2000).

[18] T. Carmon, C. Anastassiou, S. Lan, D. Kip, Z. H. Musslimani, M. Segev, and D. N. Christodoulides, Opt. Lett. **25**, 1113 (2000).

[19] W. Krolikowski, E. A. Ostrovskaya, C. Weilnau, M. Geisser, G. McCarthy, Y. S. Kivshar, C. Denz, and B. Luther-Davies, Phys. Rev. Lett. **85**, 1424 (2000).

[20] T. Carmon, R. Uzdin, C. Pigier, Z. H. Musslimani, M. Segev, A. Nepomnyashchy, and D. N. Christodoulides (unpublished).

[21] Note the distinction from quadratic solitons carrying topological charges proposed by J. P. Torres, J. M. Soto-Crespo, L. Torner, and D. V. Petrov, Opt. Commun. **149**, 77 (1998); G. Molina-Terriza, J. P. Torres, L. Torner, and J. M. Soto-Crespo, *ibid.* **158**, 170 (1998); J. P. Torres, J. M. Soto-Crespo, L. Torner, and D. V. Petrov, J. Opt. Soc. Am. B **15**, 625 (1998). There, the components are *phase related* and the nonlinearity includes terms such as ψ_1^2 and $\psi_0\psi_1^*$. In our case, all interference terms average out to zero.

[22] See, e.g., W. J. Firth and D. V. Skryabin, Phys. Rev. Lett. **79**, 2450 (1997); D. V. Skryabin and W. J. Firth, Phys. Rev. E **58**, 3916 (1998), who have shown that a scalar charge-carrying soliton disintegrates into filaments in a saturable nonlinearity. The only known exception to this are the necklace-ring solitons, which are stable self-trapped entities that exist in both Kerr and Saturable media, and can carry topological charges. See M. Soljačić, S. Sears, and M. Segev, Phys. Rev. Lett. **81**, 4851 (1998); M. Soljačić and M. Segev, *ibid.* **86**, 420 (2001). In these papers, the necklace solitons were made of a single optical field, that is, they are scalar solitons. Recently, A. S. Desyatnikov and Y. S. Kivshar have shown that composite (vector) ring solitons can be constructed as well.

[23] A. W. Snyder and J. D. Love, *Optical Waveguide Theory* (Chapman and Hall, London, 1983).

[24] The first (second) solid and dashed curves in Fig. 1(a) are jointly called the branch I (II); the first solid and second dashed curves in the same figure is called the mixed branch.

[25] J. H. Malmberg, A. H. Carlsson, D. Anderson, M. Lisak, E. A. Ostrovskaya, and Yu. S. Kivshar, Opt. Lett. **25**, 643 (2000).

[26] T. Carmon, Ph.D. thesis, Technion-Israel Institute of Technology, 2000, (unpublished).

[27] M. Segev, G. C. Valley, B. Crosignani, P. DiPorto, and A. Yariv, Phys. Rev. Lett. **73**, 3211 (1994).

[28] Demetrios N. Christodoulides and M. I. Carvalho, J. Opt. Soc. Am. B **12**, 1628 (1995).

[29] A. A. Zozulya, D. Z. Anderson, A. V. Mamaev, and M. Saffman, Europhys. Lett. **36**, 419 (1996).

[30] G. S. Garcia-Quirino, M. D. Iturbe-Castillo, J. J. Sanchez-Mondargon, S. Stepanov, and V. Vysloukh, Opt. Commun. **123**, 597 (1996).

[31] J. E. Bjorkholm and A. Ashkin, Phys. Rev. Lett. **32**, 129 (1974).

[32] A. W. Snyder and A. P. Sheppard, Opt. Lett. **18**, 482 (1993); N. V. Vysotina, L. A. Nesterov, N. N. Rozanov, and V. A. Smirnov, Opt. Spectrosc. **85**, 422 (1998); **85**, 218 (1998).

[33] The value of θ_c is different for scalar and vector solitons, since the nonlinearity necessary to generate a scalar soliton is lower than that required for a vector soliton.

[34] ϑ is given in a dimensionless units. The physical dimensional angle θ can be obtained from $\tan\theta=(2\Delta n_0/n)^{1/2}\tan\vartheta$, where Δn_0 is the maximum physical index change. Typically, $\Delta n_0/n$ is of the order of 2×10^{-4} for 10 μm FWHM solitons at $\lambda\approx0.5$ μm wavelength. The (x,y) coordinates are scaled by $(\lambda/2\pi)(n/2\Delta n_0)^{1/2}$.

[35] Z. H. Musslimani, M. Soljačić, M. Segev, and D. N. Christodoulides, Phys. Rev. Lett. **86**, 799 (2001).

[36] Y. S. Kivshar, D. E. Pelinovsky, T. Cretegny, and M. Peyrard, Phys. Rev. Lett. **80**, 5032 (1998).